Electronic Supplementary Material (ESI) for Inorganic Chemistry Frontiers.

Supporting Information (SI):

"Breathing" organic cation to stabilize multiple structures in low-dimensional Ge-, Sn-, and Pb-based hybrid iodide perovskites

Congcong Chen,[a] Emily E. Morgan,[b] Yang Liu,[a] Jian Chen,[a] Ram Seshadri[b] and Lingling Mao*[a]

a Department of Chemistry, Southern University of Science and Technology, Shenzhen, 518055, P. R. China

b Materials Research Laboratory and Materials Department, University of California, Santa Barbara, California 93106, United States

Section I. Crystallographic tables

Table S1. Crystal data and structure refinement for $(ETU)_4Ge_5I_{18}$, $(ETU)GeI_4$ and $(ETU)SnI_4$ at 298 K.

Compound	$(ETU)_4Ge_5I_{18}$	$(ETU)GeI_4$	$(ETU)SnI_4$
Formula	$C_{12}H_{44}Ge_5I_{18}N_{12}S_4$	$C_3H_{11}GeI_4N_3S$	$C_3H_{11}I_4N_3SSn$
M_r / g·mol^{-1}	3131.98	701.40	747.50
T (K)	298	298	298
Crystal System	Triclinic	Orthorhombic	Orthorhombic
Space Group	*P*-1	*Pbca*	*Pbca*
a / Å	8.6160(5)	19.178(3)	19.472(4)
b / Å	10.9195(6)	12.2635(17)	12.509(2)
c / Å	18.0200(11)	25.280(4)	25.392(4)
α / °	81.199(2)	90	90
β / °	87.561(2)	90	90
γ / °	70.561(2)	90	90
V / Å^3	1579.84(16)	5945.7(15)	6185.2(19)
Z	1	16	16
ρ_{calcd} (g·cm^{-3})	3.292	3.134	3.211
μ (mm^{-1})	11.303	10.477	9.742
F (000)	1378	4960	5248
Reflections collected	19386	41787	6325
Independent reflections	5808	5466	220
GOF on F^2	1.232	1.204	1.031
R_1, wR_2 $[I \geq 2\sigma(I)]^a$	0.0466/0.1144	0.0366, 0.0869	0.0569, 0.1046
R_1, wR_2 (all data)^b	0.0528/0.1190	0.0528, 0.0999	0.1537, 0.1392
Largest diff. peak/hole (e Å^{-3})	1.32/-4.85	2.09/-3.61	1.27/-1.65

$^aR_1 = \Sigma||F_o| - |F_c||/\Sigma|F_o|$. $^bwR_2 = [\Sigma w(F_o^2 - F_c^2)^2/\Sigma w(F_o^2)^2]^{1/2}$

Table S2. Crystal data and structure refinement for (ETU)PbI_4 at 100 K and $(ETU)_3Pb_2I_{10}$ at 298 K.

Compound	(ETU)PbI_4	$(ETU)_3Pb_2I_{10}$
Formula	$C_3H_{11}I_4N_3PbS$	$C_9H_{33}I_{10}N_9Pb_2S_3$
M_r / g·mol^{-1}	836.00	2047.02
T (K)	100	298
Crystal System	Monoclinic	Trigonal
Space Group	$P2_1/c$	R-3
a / Å	12.2987(6)	15.0135(19)
b / Å	12.5368(6)	15.0135(19)
c / Å	19.8230(10)	31.781(4)
α / °	90	90
β / °	92.204(2)	90
γ / °	90	120
V / Å^3	3054.2(3)	6203.8(18)
Z	8	6
ρ_{calcd} (g·cm^{-3})	3.636	3.287
μ (mm^{-1})	19.240	15.764
F (000)	2880	5352
Reflections collected	43292	5926
Independent reflections	5607	4081
GOF on F^2	1.024	0.985
R_1, wR_2 [$I \geq 2\sigma(I)$][a]	0.0713, 0.1898	0.0398, 0.0920
R_1, wR_2 (all data)[b]	0.0779, 0.1962	0.0581, 0.0997
Largest diff. peak/hole (e Å^{-3})	6.99/-10.76	1.84/-3.75

[a] $R_1 = \Sigma||F_o| - |F_c||/\Sigma|F_o|$. [b] $wR_2 = [\Sigma w(F_o^2 - F_c^2)^2/\Sigma w(F_o^2)^2]^{1/2}$

Table S3. Structural parameters for the low dimensional perovskites in this work.

Compounds	Space group	Metals	Δd (bond length distortion index)	σ^2 (bond angle variance)
$(ETU)_4Ge_5I_{18}$	*P*-1	Ge1	0.00522	6.3326
		Ge2	0.05874	11.3104
		Ge3	0.06004	18.8684
$(ETU)GeI_4$	*Pbca*	Ge1	0.08157	27.3030
		Ge2	0.08235	23.7656
$(ETU)SnI_4$	*Pbca*	Sn1	0.02521	6.4817
		Sn2	0.03848	19.0447
$(ETU)PbI_4$	$P2_1/c$	Pb1	0.01091	3.0167
		Pb2	0.01460	7.6529
$(ETU)_3Pb_2I_{10}$	*R*-3	Pb1	0.00850	16.2803
		Pb2	0.00000	95.8555
		Pb3	0.00000	0.7449

Table S4. M-I-M angles in $(ETU)_4Ge_5I_{18}$, $(ETU)GeI_4$, $(ETU)SnI_4$, $(ETU)PbI_4$ and $(ETU)_3Pb_2I_{10}$.

Compound	Labels	Angles (°)
$(ETU)_4Ge_5I_{18}$	Ge(1)-I(2)-Ge(2)	161.88(3)
	Ge(2)-I(7)-Ge(3)	68.49(3)
	Ge(2)-I(6)-Ge(3)	75.96(3)
	Ge(2)-I(1)-Ge(1)	171.39(3)
	Ge(2)-I(5)-Ge(3)	78.04(3)
$(ETU)GeI_4$	Ge(1)-I(7)-Ge(2)	162.14(3)
	Ge(2)-I(5)-Ge(1)	162.06(3)
	Ge(2)-I(6)-Ge(2)	157.40(3)
	Ge(1)-I(3)-Ge(1)	167.58(4)
$(ETU)SnI_4$	Sn(2)-I(3)-Sn(1)	167.06(5)
	Sn(2)-I(7)-Sn(2)	168.39(6)
	Sn(1)-I(1)-Sn(2)	159.25(5)
	Sn(1)-I(2)-Sn(1)	155.42(5)
$(ETU)PbI_4$	Pb(2)-I(2)-Pb(1)	146.06(5)
	Pb(1)-I(3)-Pb(1)	154.50(5)

Section II. Simulated and experimental powder X-ray diffraction (PXRD) patterns

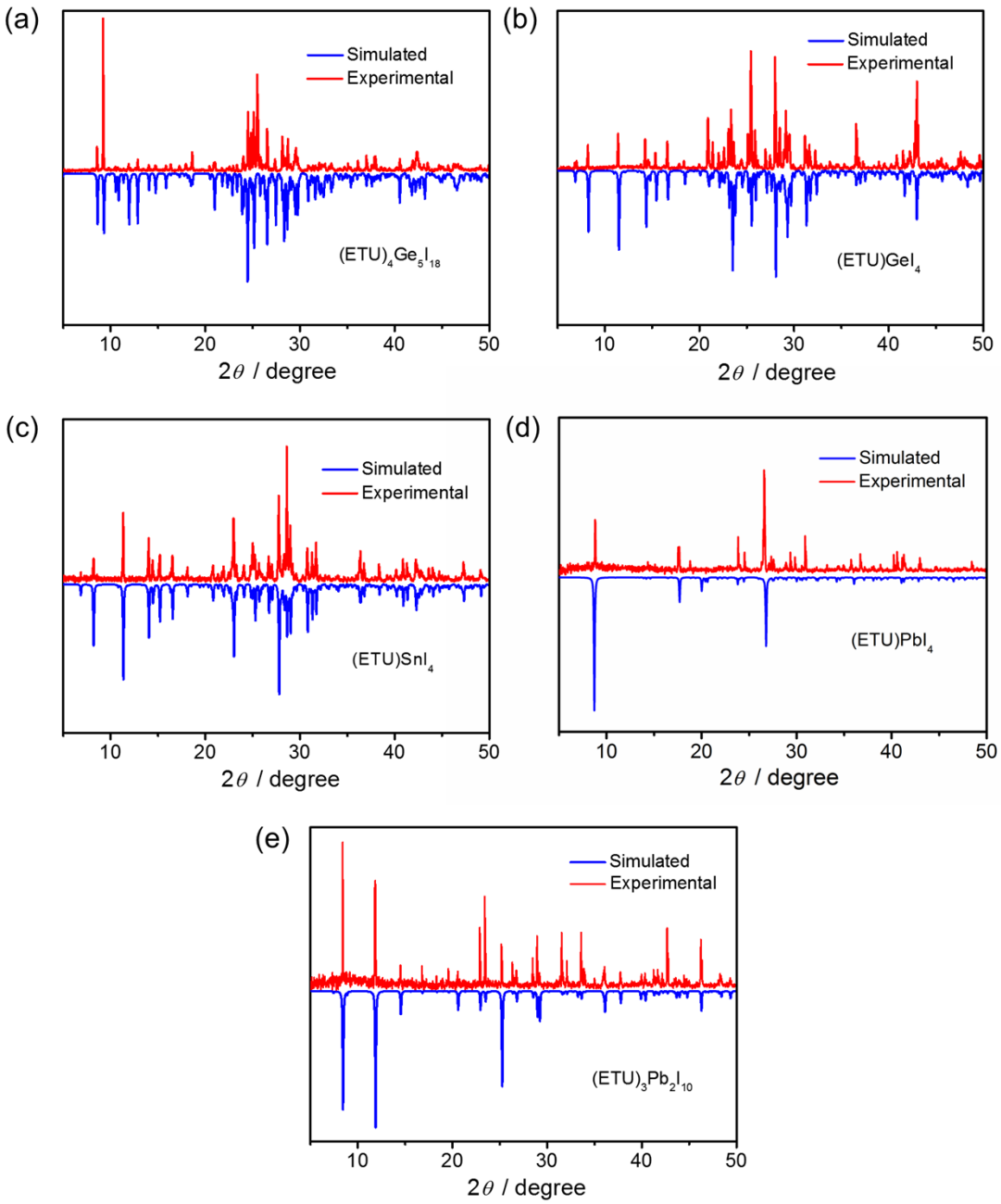

Fig. S1 Comparison of the experimental and simulated PXRD patterns for $(ETU)_4Ge_5I_{18}$ (a), $(ETU)GeI_4$ (b), $(ETU)SnI_4$ (c), $(ETU)PbI_4$ (d) and $(ETU)_3Pb_2I_{10}$ (e). Due to the large size of the crystal in test for $(ETU)PbI_4$, the crystal anisotropy along the (110) crystal face is more prominent.

Section III. Extra structural illustrations

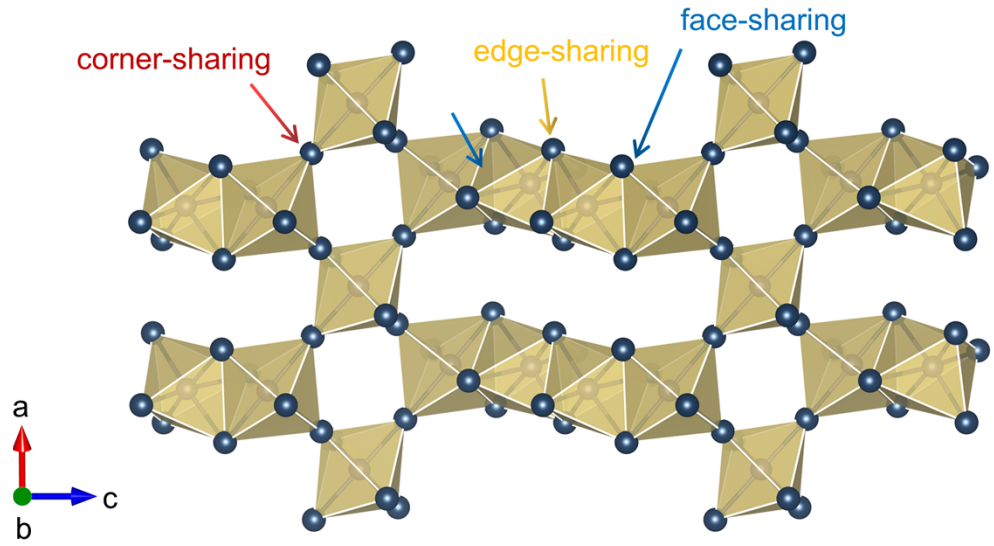

Fig. S2 Inorganic layer configuration of $(ETU)_4Ge_5I_{18}$ along the b axis. Arrow symbol: blue (face-sharing), yellow (edge-sharing), red (corner-sharing).

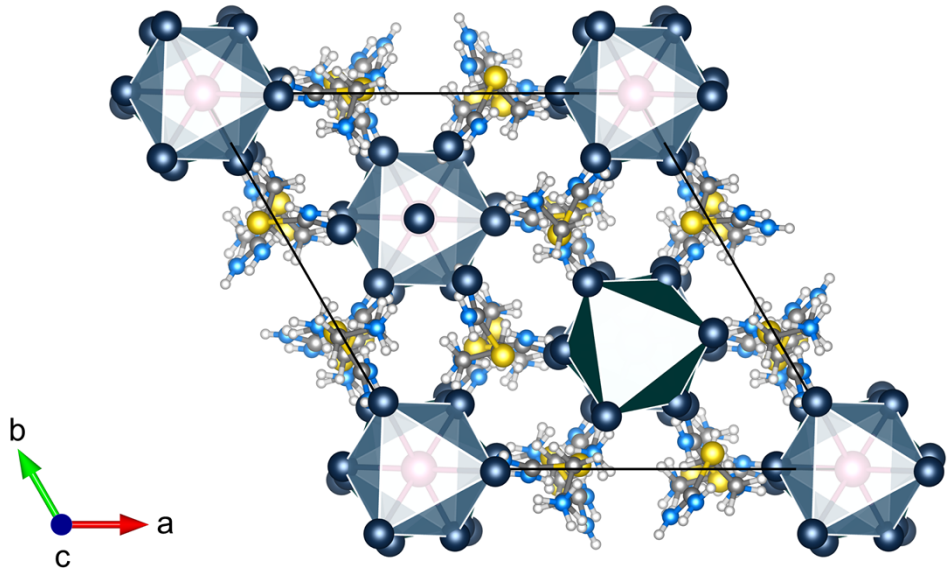

Fig. S3 Crystal structures of $(ETU)_3Pb_2I_{10}$ along the c axis.